



## A Study on Quantitative Assessment of Crack Tip Constraint by 'Q' Parameter

T. V. Pavankumar, J. Chattopadhyay, B. K. Dutta and H. S. Kushwaha

*Bhabha Atomic Research Centre, India*

**ABSTRACT** - Recent advances highlight the loss of J-dominance in low constraint geometries and the importance of using two parameter theories, namely J-T and J-Q to characterise near crack tip stress states of crack geometries. In this paper, the behaviour of Q-value as constraint parameter is investigated using 2D finite element models of center cracked panel, three point bend bar and compact tension specimen geometries. It is identified that Q-parameter can be used along with the J-integral to fully characterise the crack-tip stress state. It is independent of distance over the range of  $J/\sigma_0$  to  $5J/\sigma_0$  for low constraint geometries. For a given material, there exists a unique linear relationship between triaxiality factor (h) and Q-value for low constraint geometries.

### INTRODUCTION

Crack initiation and stable crack growth in ductile materials are usually described by J-R curves obtained from standard fracture specimens. The original idea was that a single parameter, J-integral can be used to characterise the crack tip stress field and one unique fracture resistance curve is sufficient to characterise the material. However, there is growing evidence showing that the J-R curve depends on specimen size, geometry and loading mode. Therefore, the transferability of specimen J-R curve to component level is an unresolved issue that currently receives a lot of attention among researchers. The influence of crack tip constraint or stress triaxiality on ductile fracture has been emphasised recently in explaining the geometry dependent fracture resistance of specimens and structures to ductile tearing [1,2]. Generally, the standard laboratory specimens are high constraint geometries. However, the real structures may be low constraint geometries. Hence, use of toughness properties from high constraint geometries to low constraint geometries introduces a large degree of conservatism in the design. On the other hand, the application of toughness properties from low constraint specimen geometries to the structural applications with high constraint crack geometries leads the design unsafe.

Recent advances highlight J-Q theory [3] to characterise the near crack tip stress states of yielded crack geometries. In this theory, the J-integral is retained as a measure of the crack-tip deformation state, while the second parameter 'Q' is added to quantify the crack tip constraint. As per this theory, the laboratory specimen must match the constraint of the component i.e. two

geometries must have the same Q-value at failure in order to have the same  $J_c$  values. The nondimensional parameter 'Q' is defined as,

$$Q = [\sigma_{\theta\theta} - (\sigma_{\theta\theta})_{ref}] / \sigma_0 \text{ at } \theta = 0^\circ-90^\circ, r=2J / \sigma_0, \quad (1)$$

where, r and  $\theta$  are polar co-ordinates situated at the crack-tip.  $\sigma_{\theta\theta}$  is the existing stress field ahead of the crack-tip of the actual geometry,  $(\sigma_{\theta\theta})_{ref}$  is the reference solution obtained from the standard plane strain small scale yielding solution  $(\sigma_{ij})_{SSY, T=0}$ .

A negative (positive) Q-value means that the hydrostatic stress is lower (higher) than the reference field (Q = 0 state). Geometries with negative Q-value show low stress triaxiality ahead of the crack tip and loss of J-dominance, while geometries with  $Q \geq 0$  show high triaxiality ahead of crack tip and good agreement with the HRR[4,5] or SSY fields. Thus, the Q-value provides a framework for quantifying the determination of constraint as plastic flow progresses from small scale yielding to fully yielded conditions [3].

In this paper, the characteristics of Q-value are studied using two dimensional elastic-plastic finite element models of finite width specimens. The specimens studied are Centre Cracked Panel (CCP), Three point bend bar (TPBB) and Compact Tension specimen (CT) for a range of a/w ratios and strain hardening exponents (n). The analysis has also been carried out for Indian PHWR PHT (Primary Heat Transport) piping material. The main aim of this paper is to study the characteristics of the Q-value as a constraint indexing parameter, and its relationship with the triaxiality factor (h). These data will be used in transferring the laboratory specimen J-R curve to the component level considering the crack-tip constraint. The components of interest here include cracked straight pipe and elbow of the primary heat transport system of nuclear power plants.

## FINITE ELEMENT ANALYSIS

Two dimensional plane strain finite element analyses are conducted to obtain very detailed resolution of the crack tip stress fields for the modified boundary layer (MBL) model and CCP, TPBB, CT geometries. The numerical models employ conventional small strain theory. The finite element program, ABAQUS [6] is used to analyse the finite element models presented in this paper. The remainder of this section outlines the details of the models beginning with those aspects common to MBL, CCP, TPBB and CT analyses.

### Material Parameters

The material model employs  $J_2$  deformation plasticity theory. The uniaxial stress-strain curve follows Ramberg-Osgood form

$$\varepsilon/\varepsilon_0 = \sigma/\sigma_0 + \alpha (\sigma/\sigma_0)^n \quad (2)$$

where,  $\varepsilon$  is the true strain,  $\sigma$  is the true stress,  $\sigma_0$  is yield stress,  $\varepsilon_0 = \sigma_0/E$ , E is Young's modulus,  $\alpha$  is the Ramberg-Osgood coefficient and n is the strain hardening exponent.

Different strain hardening exponents, n=3,5,10&20 are chosen which cover the range of steels from high strain hardening to ideal plastic materials. The parameter  $\alpha$  is assigned a value of '1' for a piecewise power-law material. The other properties typical of those for a moderate

strength steel are adopted in the computation ( $\epsilon_0=1/500$ ,  $\sigma_0=400\text{MPa}$ , and  $\nu=0.3$ ). The analysis has also been carried out for Indian PHWR PHT piping material (SA 333 Gr6). The material properties at the temperature of  $250^\circ\text{C}$  [7] are as follows.  $\sigma_0=240\text{MPa}$ ,  $E=188\text{GPa}$ ,  $n=3.273$  and  $\alpha = 8.1505$ .

#### The Modified Boundary Layer Model

The reference field in Eq.(1) is computed by means of a standard boundary layer solution mentioned earlier. For this purpose, a focused mesh (half circular) having outer boundary radius 'R' is used. On the boundary of this model displacements corresponding to elastic solution are applied. This analysis is referred as Modified Boundary Layer (MBL) analysis, which simulates near-tip conditions in an arbitrary geometry provided plasticity is well contained within the boundary. These models each contain 1200 elements and 3741 nodes. Eight noded isoparametric quadrilateral elements are used throughout. Reduced integration is employed in the analysis. These models had 30 elements in the circumferential and 40 elements in radial direction, respectively. The model is loaded by imposing displacement increments of the elastic singular field for mode I on the outer circular boundary.

$$\Delta u(r,\theta)=(1+\nu)\Delta K_I (\tau/2\pi)^{0.5}(3-4\nu-\cos \theta) \text{Cos}(\theta/2)/E \quad (3)$$

$$\Delta v(r,\theta)=(1+\nu)\Delta K_I (\tau/2\pi)^{0.5}(3-4\nu-\cos \theta) \text{Sin} (\theta/2)/E \quad (4)$$

SSY solutions are enforced by not allowing the plastic zone size beyond  $0.01R$ . Reference stresses have been calculated at a distance of  $cJ/\sigma_0$  ( $c=1,2,3,4,5$ ) ahead of crack-tip at different circumferential positions ( $\theta = 0^\circ - 90^\circ$ ) around the crack tip.

#### Numerical Modelling of Specimens

Fig.(1) shows schematic drawings of typical CCP,TPBB and CT specimens used in the current study. Due to symmetry in both geometry and loading conditions, only  $1/4^{\text{th}}$  of the CCP, half of TPBB and half of CT are modelled. Different finite element models are constructed for each of  $a/w$  ratios investigated. Eight noded plane strain isoparametric quadrilateral elements have been used. Reduced ( $2 \times 2$ ) Gaussian integration is used to eliminate locking of arbitrarily shaped elements. A half circular core of elements surrounding the crack tip is common to all models. This core consists of 20 elements in circumferential direction and 30 elements in radial direction. A typical finite element mesh showing a close up zone at the crack front region is given in Fig.(2). Each mesh consists of 3308 nodes and 1047 elements.

#### RESULTS AND DISCUSSION

A large number (60) of analyses were conducted. However, a small portion of the results have been presented here. Some key results are shown in Figs.3-7. All the Q-values, triaxiality factor are evaluated at  $\theta=0^\circ$  unless otherwise stated.

Figs.(3a&3b) show the variation of Q with increasing deformation level for shallow ( $a/w=0.1$ ) and deeply cracked ( $a/w \geq 0.5$ ) geometries for Indian PHWR PHT piping material respectively. The deformation level ( $J/\sigma_0$ ) is normalised by crack length 'a' for  $a/w \leq 0.5$  and by ligament length 'b' for  $a/w \geq 0.5$ . It may be noted that the constraint loss is gradual with

increasing deformation level irrespective of specimen geometry in the case of shallow cracked geometries as is evident from Fig.3a. Q-values are negative for these geometries and these can be treated as low constraint geometries. Referring to Fig.3b deeply cracked TPBB and CT specimens stay close to the Q=0 state (high constraint geometry) to fairly high deformation levels ( $J/(b\sigma_0) \approx 0.02$ ) and thereafter decreases rapidly. However, the behaviour of deeply cracked CCP is same as that of shallow cracked geometry. Referring to Figs.3a&3b, it is noted that CT specimen maintains high crack tip constraint than the other two specimens for the same a/w ratio. Whereas, CCP maintains low crack tip constraint than the other two specimens.

Figs.4a&4b show effect of strain hardening on Q for shallow cracked (a/w = 0.1) and deeply cracked (a/w=0.5) CT geometries respectively. It may be noted that the effect of strain hardening on 'Q' is significant on shallow cracked geometry which is a low constraint geometry. In contrast, its effect is weak for deeply cracked geometry (high constraint geometry) as shown in Fig.4b.

Figs.5a&5b shows variation of Q with distance. Q is evaluated at the distance of  $cJ/\sigma_0$  (c=1,2,3,4,5) ahead of crack tip. Referring to Fig.5a, it is observed that Q is independent of distance at low load levels and has slight dependence on distance at high load levels in the case of shallow cracked CT geometry. In contrast, it is dependent on distance in the case of deeply cracked CT geometry at high load levels as is evident from Fig.5b. Fig.6a&6b shows the variation of Q along circumferential direction for CT specimen. Q values are evaluated at a distance of  $2J/\sigma_0$  from the crack-tip at  $\theta=0^\circ$  to  $90^\circ$ . It is noted that 'Q' value decreases with the increase in ' $\theta$ ' for shallow cracked geometry as is evident from Fig.6a. Whereas, it is nearly constant along circumferential direction for deeply cracked CT geometry (Fig.6b).

Fig.7 shows the variation of triaxiality factor, h with Q. The triaxiality factor 'h' can also be used as constraint indexing parameter. It is defined as the ratio of hydrostatic or mean stress ( $\sigma_m$ ) to the Mises equivalent stress ( $\sigma_e$ ). Both 'h' and 'Q' are evaluated at a distance of  $2J/\sigma_0$  from the crack-tip. It may be noted that the triaxiality factor decreases as Q decreases as is evident from the Fig.7. For low constraint geometries, unique linear relationship can be obtained for a given material, irrespective of crack depth. The following relationship has been obtained for Indian PHWR PHT piping material (SA 333 Gr6).

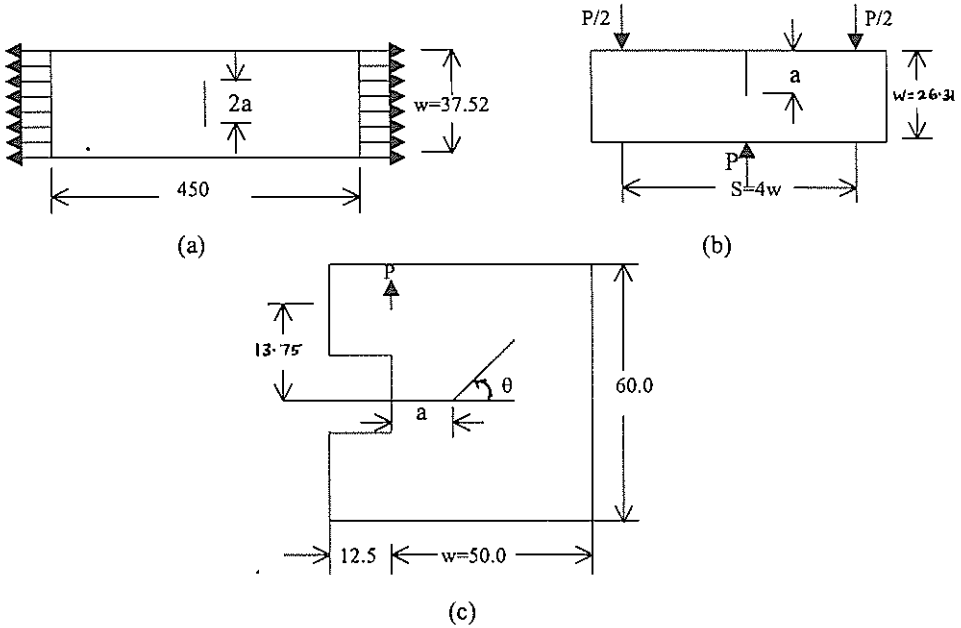
$$h = 3.44084 Q + 4.36815 \dots\dots\dots(5)$$

## CONCLUSIONS

This study examined the characteristics of constraint indexing parameter, Q. Based on the results it is identified that Q-value can be used to quantify the crack tip constraint. It is observed that the crack tip constraint loss is gradual with increasing deformation levels in the case of CCP geometries and shallow cracked TPBB and CT geometries. Q-values for these geometries are increasingly negative with the deformation levels. Q-values stay close to zero for deeply cracked TPBB&CT geometries and hence these can be treated as high constraint geometries for which single parameter characterisation is valid. Q-values show slight dependence on 'r' ( $J/\sigma_0$  to  $5J/\sigma_0$ ) at fully yielded solutions for low constraint geometries. Q-value is nearly independent of ' $\theta$ ' for high constraint geometries. It is found that for a given material, there exists a unique linear relationship between triaxiality factor and 'Q' for low constraint geometries.

References

1. Brocks, W., Kunecke, G., Noack, H.D., & Veith, H., "On the transferability of Fracture Mechanics to Structures using FEM", Nuclear Engineering and Design, Vol.112,1989,pp.1-14.
2. Schuler, X., Blind, D., Eisele, U., Herter, K.H., & Stoppler, W., "Fracture Mechanics Evaluation of Cracked Components with Consideration of Multiaxiality of Stress State", Nuclear Engineering and Design, Vol. 151, 1994, pp. 29-305.
3. O'dowd, N.P. and Shih, C.F., "Two parameter Fracture Mechanics: Theory and Applications", NUREG/CR-5958, 1993.
4. Hutchinson, J.W., "Singular behaviour at the end of a tensile crack tip in a Hardening Material", Journal of Mechanics and Physics of Solids, Vol.16,1968, pp.13-31.
5. Rice, J.R. and Rosengren, G.F., "Plane Strain Deformation near a Crack Tip in a Power Law Hardening Material", Journal of Mechanics and Physics of Solids, Vol.16,1968, pp.1-12.
6. Hibbitt, Karlsson and Sorensen, Inc., ABAQUS, User's manual, Theory Manual , Verification and Example problems , Version 5.2, 1992.
7. Singh, P.K., Chattopadhyay, J. & Kushwaha, "Tensile and fracture properties evaluation of PHT system piping material of PHWR", International Journal of Pressure Vessel and Piping, Vol.75, pp 271-280, 1998.



Note: All dimensions are in mm

Fig.1 Schematic drawings of 2D geometries (a) Centred Cracked Panel (b) Three Point Bend Bar (c) Compact Tension Specimen

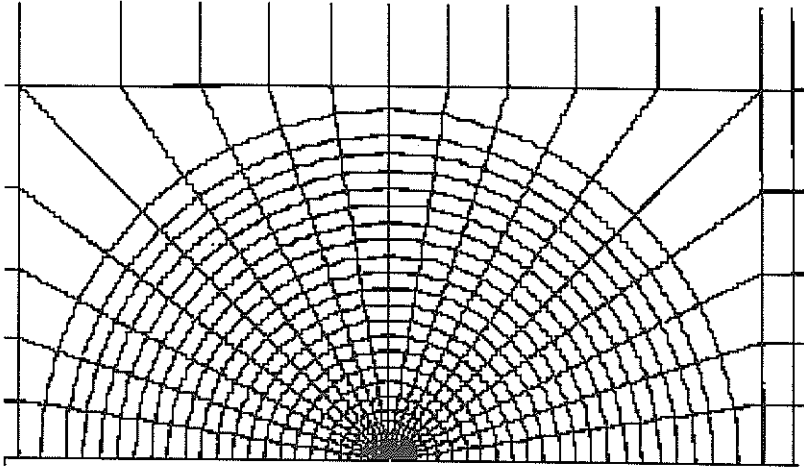


Fig.2 Finite Element Mesh showing details of Crack Tip region

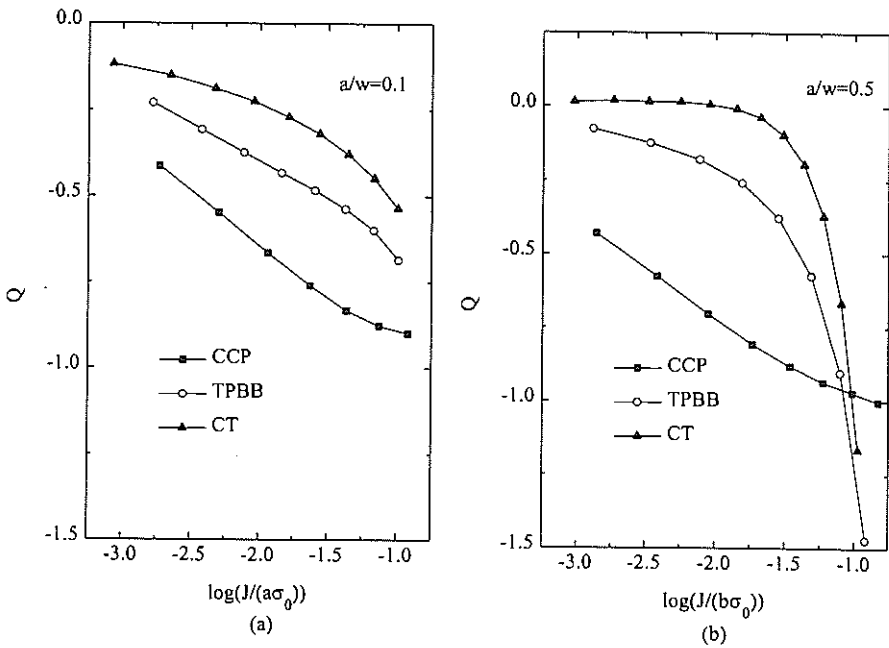


Fig.3 Variation of 'Q' with deformation level for SA333 Gr6 steel

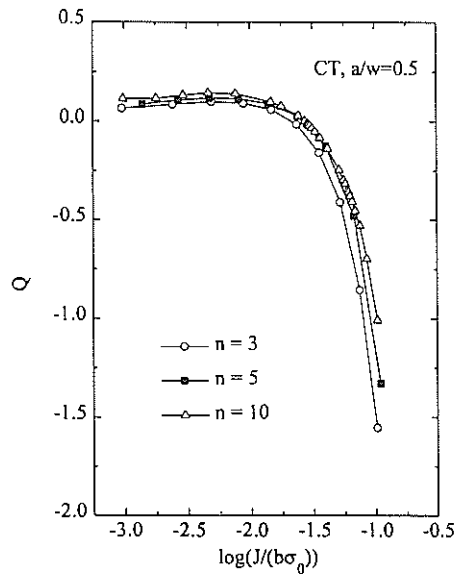
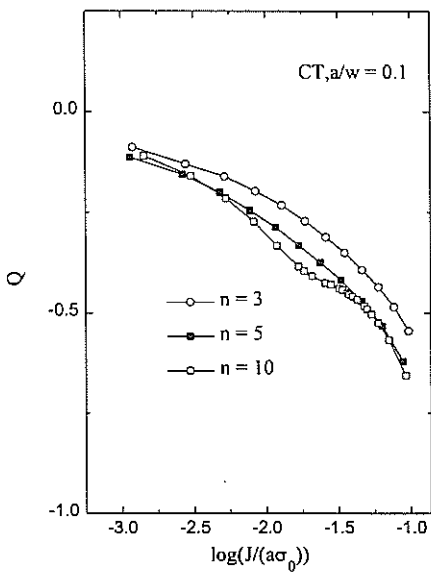


Fig.4 Effect of strain hardening on 'Q'

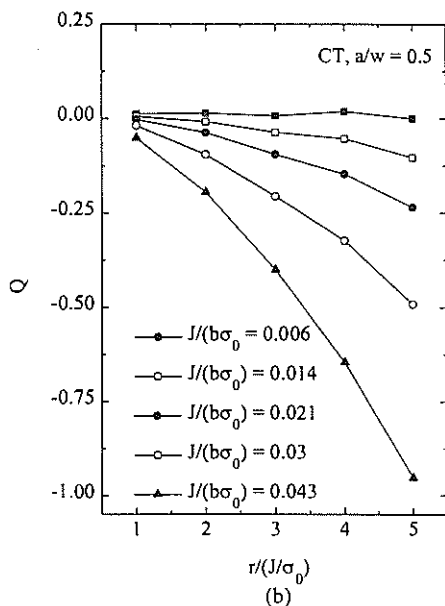
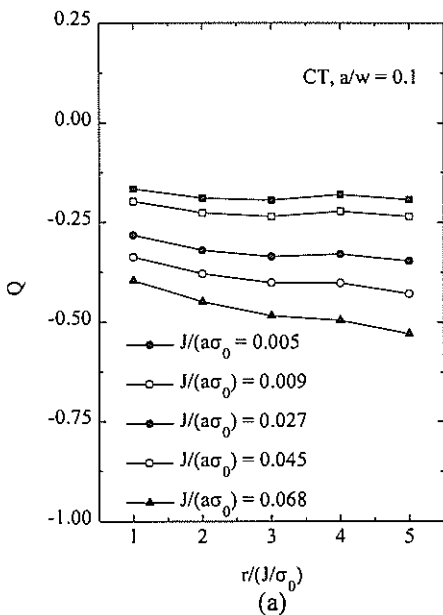


Fig.5 Variation of 'Q' with distance ahead of crack tip for SA333 Gr steel

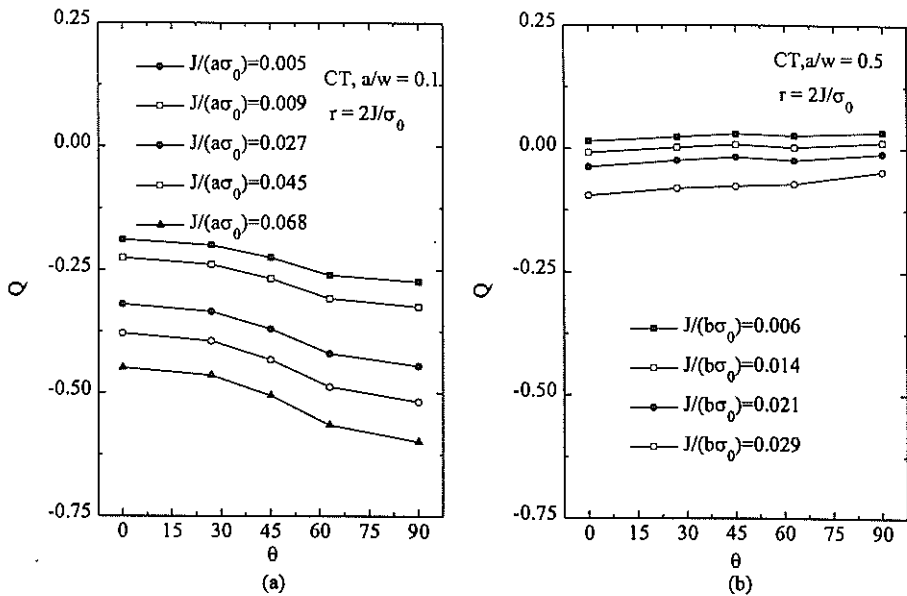


Fig.6 Variation of 'Q' along circumferential direction(SA 333 Gr6)

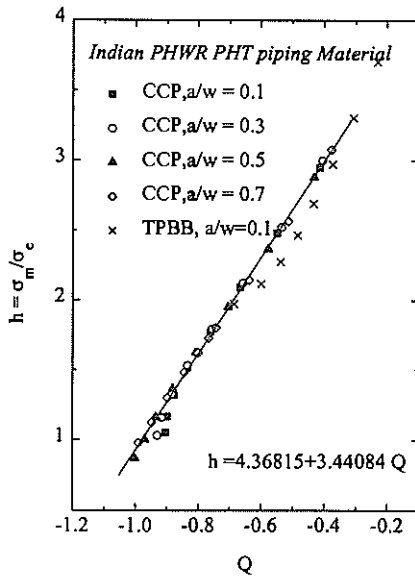


Fig.7 Variation of h with Q, for low constraint geometry